Biomaterials Science

Characterizing the encapsulation and release of lentivectors and adeno-associated vectors from degradable alginate hydrogels

Journal:	*Biomaterials Science*
Manuscript ID	BM-ART-10-2018-001218.R1
Article Type:	Paper
Date Submitted by the Author:	27-Nov-2018
Complete List of Authors:	Madrigal, Justin; University of California Davis, Biomedical Engineering Shams, Shahin; University of California Davis, Biomedical Engineering Stilhano, Roberta; University of California Davis, Biomedical Engineering; University of Sao Paulo, Biochemistry Silva, Eduardo; University of California Davis, Biomedical Engineering

Characterizing the encapsulation and release of lentivectors and adeno-associated vectors from degradable alginate hydrogels

Justin L. Madrigal[1*], Shahin Shams[1*], Roberta S. Stilhano[1,2] and Eduardo A. Silva[1]

[1]Department of Biomedical Engineering, University of California, Davis, CA, USA.

[2]Department of Department of Biochemistry, University of Sao Paulo, Sao Paulo, Brazil.

* - These authors contributed equally to the current study.

Corresponding author:

Eduardo A. Silva

Department of Biomedical Engineering

1 Shields Ave.

Davis, CA, USA 95616

Email: esilva@ucdavis.edu

Phone: 1-530-754-7107

Fax: 1-530-754-5739

ABSTRACT

Gene therapy using viral vectors has been licensed for clinical use both in the European Union and the United States. Lentivectors (LV) and adeno-associated vectors (AAV) are two promising and FDA approved gene-therapy viral vectors. Many future applications of these vectors will benefit from targeting specific regions of interest within the body. Therefore, building on the early success of these vectors may depend on finding effective delivery systems to localize therapeutic administration. Degradable alginate hydrogels have been tested as appealing delivery vehicles for the controlled delivery of vector payloads. In this study, we compare the ability of two different degradable alginate hydrogel formulations to efficiently deliver LV and AAV. We propose that release rates of viral vectors are dependent on the physical properties of both the hydrogels and vectors. Here, we demonstrate that the initial strength and degradation rate of alginate hydrogels provides levers of control for tuning LV release but do not provide control in the release of AAV. While both alginate formulations used showed sustained release of both LV and AAV, LV release was shown to be dependent on alginate hydrogel degradation, while AAV release was largely governed by diffusive mechanisms. Altogether, this study demonstrates alginate's use as a possible delivery platform for LV and, for the first time, AAV – highlighting the potential of injectable degradable alginate hydrogels to be used as a versatile delivery tool in gene therapy applications.

KEY WORDS: gene therapy; biomaterials; AAV; degradable polymers; delivery systems

INTRODUCTION

Since August 2017 gene therapy is FDA approved for clinical application. The three FDA approved therapies utilize two viral vectors – lentivectors (LV) and adeno-associated vectors (AAV). Despite the clinical success of these viral vectors, barriers to their use *in situ* still exist. LV therapies currently approved are *ex vivo* manipulations of cells, but the high costs, complexity, and limited tissue targets of this approach motivate the need for *in situ* LV therapies to be developed. LV gene therapies in general integrate their genetic payloads directly into the chromosome of the host cell, and retain any modification following cellular division. This is beneficial for ensuring long term expression of the target gene through multiple generations of proliferative cells or non-proliferative cells alike (1–4). However, off target cell transduction presents a persistent biosafety hazard for proposed *in situ* LV therapies, and this necessitates strategies for localizing the delivery of LV to target tissue. In contrast, AAV genetic payloads remain largely episomal and do not replicate along with the host genome. In non-dividing cells highly stable episomes allow for extended windows of expression, whereas the effects will diminish over time in regions with high cell turnover or replication (5). Similar to LV, the persistence of potential expression in non-dividing cells calls for the utility of controlled delivery of AVVs. In addition, AAVs can be quickly neutralized by the body since the major serotypes are frequently encountered by the human population in the wild (6). This motivates the need for delivery approaches that can protect the vector from viral clearance. Altogether, the nature of both of these vectors motivates the use of a biomaterial system as a controlled delivery device to improve both the biosafety and efficacy of these therapies.

A variety of natural and synthetic biomaterials have been studied for controlled release of many payloads, including gene therapies. Hydrogels are an especially appealing class of delivery vehicles for clinical applications of genetic cargos as they can be introduced into the body with minimally invasive procedures. Fibrin (7,8), PEG (9,10), and self-assembling peptide hydrogels (11,12) have been shown to successfully encapsulate and release both AAV and LV. However, each study focused on single viral vectors and never directly compared AAV and LV within the same biomaterial system. Alginate, a negatively charged biomaterial, it is an attractive and versatile (1,13,14) vehicle that has also been tested for the delivery of viral vectors due to its low immunogenicity, tunable biodegradability, and gentle gelation procedure (1,15,16). In contrast with other hydrogels used for viral delivery, alginate is particularly appealing for applications where transduction is intended to be obtained outside the polymer network *in situ* directly within the cellular microenvironment of the tissue target without tissue interaction. Alginate hydrogels are well known for the not supporting cell infiltration and adhesion without chemical modifications (17,18). Typically, the release of payloads from alginate hydrogels can be tuned by controlling three key aspects of an alginate hydrogel system: i) the diffusivity of the payload within the hydrogel; ii) the degradability of the hydrogel; and iii) the affinity between the alginate and the payload. The three aspects above have been used to control the release of small molecules, proteins, and, more recently, larger particles such as viral vectors (1,19,20).

AAV and LV display distinct intrinsic physical characteristics, including divergent sizes and surface features (Table 1). Given these differences it is expected that the mechanism of release from alginate hydrogels vectors will differ between the two vectors.

For example, the mesh size a key characteristic of alginate hydrogels that influences diffusivity. Indeed, the reported alginate hydrogel pore sizes range from ~5 - 170 nm and therefore for cargos that display similar sizes disruption of the existing polymer network (i.e. degradation) it is necessary to modulate the cargo release (1,21). Alginate hydrogels can be engineered to degrade on a scale that ranges from days to months by varying the alginate molecular weight composition, mismatch in the size of cross-linking junctions and degree of polymer chain oxidation (1,22,23). Therefore, degradable alginate hydrogels are desirable delivery vehicles that can be tailored to meet desired release rate of viral vectors such as LV and AAV.

In this manuscript, we investigated how alginate hydrogels were found to encapsulate and release two types of viral vectors, LV and AAV. We hypothesized that these vectors would maintain their activity through encapsulation and release, and that hydrogel degradation could be used to further enhance release and transduction. We first compared the transduction potential of our specific vectors in suspension and compared their stability in different environments and over time. The release profile and gene expression potential of viral-loaded hydrogels was compared for two formulations of alginate that differ in their degradability. Through this process we have shown that these two clinically approved viral vectors can be delivered using alginate hydrogels - but that the mechanism with which they were delivered differed starkly between them. LV particles were dependent on hydrogel degradation to be released, and therefore the alginate hydrogel formulation's degradation rate corresponded to release rate of the LV particles. In contrast, AAV release was controlled by diffusive action and was independent of degradation of the alginate hydrogel used. While degradable alginate hydrogels have

been previously shown to successfully encapsulate and release LV (1,15), to our knowledge this is the first study looking at AAV release from degradable alginate hydrogels. In addition, we believe that this is the first study that directly compares the release of these two viral vectors from the same hydrogel formulations. Our results suggest that degradable alginate hydrogels are capable of sustained release of not only functional LV particles but AAV particles as well, albeit by different mechanisms. This controlled release of vectors of drastically different sizes and biochemistries from degradable alginate hydrogels demonstrates the expanding therapeutic potential of using alginate biomaterial platforms for gene therapy approaches.

MATERIALS & METHODS

Viral Vectors

Lentivectors were produced using the plasmids pLV-CMV-hCXCL12-IRES-DsRed (transfer vector driving red fluorescent protein (DsRed) reporter genes from a universal immediate early CMV promoter), psPAX2 (Addgene) and pCMV-VSV-G (Addgene) were used to produce the lentivectors. Viral vector production, concentration, and titration were performed following established protocols (2). In brief, lentivectors were produced in human embryonic kidney (HEK-293T) (ATCC) cells cultured in Dulbecco's modified Eagle's medium (DMEM; Invitrogen) with 10% fetal bovine serum (FBS; Invitrogen) and 1% penicillin-streptomycin (Invitrogen) (DMEMc) at 37˚C and under 5% CO_2. HEK-293T cells were transfected using the calcium phosphate co-precipitation method. All transfer vectors - LV with CMV driving DsRed and AAV serotypes 1 and 2 with CMV driving blue fluorescent protein (BFP) and enhanced green fluorescent protein (EGFP) were packaged by and purchased from Vector Builder (Cyagen).

Alginate formulations and hydrogel preparation

Alginate hydrogels were prepared using two stock alginates, Protanal LF10/60 and LF20/40 (Novamatrix), as low and high molecular weight polymers respectively. These alginates were used, without modification, for an unoxidized source of alginate. Oxidized alginates were produced through a reaction with sodium periodate ($NaIO_4$) (Sigma Aldrich) to partially oxidize either 1% or 5% of the uronate monomers as previously described (1,24). Briefly, alginate polymers were diluted to 1% w/v in ddH_2O overnight. The molar ratio of alginate monomers and $NaIO_4$ was calculated and adjusted accordingly (21 mg and 108 mg of $NaIO_4$ necessary for, respectively, oxidizing 1% and 5% of the

sugar residues). 1% and 5% of the sugar residues in the polymer chains were oxidized by mixing the alginates solutions with an aqueous solution of $NaIO_4$ while maintaining solutions in the dark for 17 hours at room temperature. An equimolar amount of ethylene glycol (Fisher) was then added to stop the reaction, and the solution was subsequently dialyzed (MWCO 3500, Spectra/Por®) over 3 days. The solution was sterile filtered, frozen (-20˚C overnight), lyophilized and stored at –20˚C. From this set of both unoxidized and oxidized alginates, two general formulations were used for all studies unless otherwise mentioned. First, 1% oxidized LF10/60 and 1% oxidized LF20/40 were combined at a 75:25 ratio to create a slow degradation formulation. Secondly, 5% oxidized LF20/40 and nonoxidized LF10/60 were combined at an 80:20 ratio to create a fast degradation formulation.

To prepare hydrogels, sterile solutions of alginate were ionically crosslinked using an internal gelation strategy based on the reaction of calcium carbonate ($CaCO_3$, SkySpring Nanomaterials) and glucono delta-lactone (GDL, Sigma Aldrich). Alginate (final concentration 2%) was mixed with $CaCO_3$, then GDL (final respective concentrations 140mM and 70mM) and then cast into molds (8mm diameter, 1.5mm height, or 6 mm, 1.5 mm height) for 1.5 hours to allow for full gelation. Hydrogels were then collected and used immediately for all studies. Viral vectors were encapsulated within hydrogel disks by mixing the vector of interest into the pre-crosslinked alginate polymer solutions. Each component is individually added and thoroughly mixed during the gelation procedure – therefore, by adding the virus of interest to the alginate solution prior to the addition of the crosslinking agents, homogenous distribution of viral particles in the hydrogel disks is ensured.

Rheologic and degradation characterization of hydrogel disks

Measurements of storage and loss shear moduli were performed using a Discovery HR3 hybrid rheometer (TA instruments) with an 8-mm parallel-plate geometry in time frequency and strain sweep modes. Slow and fast degradation formulation hydrogels were prepared as described above and swollen overnight in phosphate buffered saline supplemented with calcium and magnesium ions (PBS^{++}, Invitrogen). Following swelling, hydrogels were incubated for the remainder of the study in cell culture conditions at 37˚C. At select time points the storage modulus, swelling ratio, mesh size, and dry mass of hydrogel disks were assessed. The linear viscoelastic region of these hydrogel disks was determined via frequency and strain sweep analysis of fully crosslinked hydrogels. Strain sweeps were then performed within the linear viscoelastic region at a strain of 0.1%, and a frequency of 1 rad/s, and a temperature of 23˚C to obtain the storage modulus. The difference in incubation (37˚C) and strain sweep (23˚C) reading temperatures has negligible effect on measurements recorded. The degree of swelling, Q, was defined as the reciprocal of the polymer volume fraction in the hydrogel (v_2):

$$v_2 = \frac{1}{\rho_P}\left(\frac{Q_m}{\rho_w} + \frac{1}{\rho_P}\right)^{-1} \qquad [1]$$

$$Q = {v_2}^{-1} \qquad [2]$$

Here, ρ_P is the density of alginate (1.515 g cm^{-3}), ρ_w is the density of water, and Q_m is the swelling ratio of wet mass over dry mass for the hydrogels (25).

Hydrogel mesh size was estimated as previously described using swelling and rheometry data. Molecular weight between crosslinks (M_c) was calculated from the shear modulus elastic component (G', Pa) using the following equation:

$$M_c = C_p RT/G' \qquad [3]$$

where C_p is the alginate concentration, R is the gas constant, and T is the temperature at which the measurement was taken. Characteristic mesh size (ξ) was calculated as follows:

$$\xi = v_2^{-1/3} l \left(2\frac{M_c}{M_r}\right)^{1/2} C_n^{1/2} \qquad [4]$$

where l is the length of the repeating unit (5.15 Å), M_r is the molecular weight of the repeating unit (194 g mol^{-1}), and C_n = 0.021M_n+ 17.95 = 21.1 (15).

Titration of viral vectors and continuous culture

HEK-293T cells were transduced with a range of concentrations of either AAV or LV. After 3 days, the transduced cells were analyzed for either BFP, EGFP, or DsRed expression for AAV, or LV, respectively, using an Attune flow cytometer (Thermo Fisher) (>25,000 events analyzed) and the respective titer of each vector was calculated.

Following titration, new HEK-293T cells were transduced using a consistent multiplicity of infection (MOI) between viral vectors (MOI= 20, 10, or 2) and the resulting transduction efficiency was analyzed using flow cytometry (n=3). These transduced cells were then passaged and cultured for three additional days, at which point they were again collected and analyzed using flow cytometry to measure residual levels of fluorophore expression.

Viral vector stability in suspension and encapsulation

Viral vector suspensions (MOI = 10) and hydrogel disks encapsulating viral vectors (MOI of each disk = 40) were incubated in DMEMc at 37˚C for increasing time prior to

addition to cells. For this experiment, hydrogels were composed of unoxidized LF10/60 and LF20/40 alginates at a 75:25 ratio. At 0, 14, 25, 52 hours, viral vector suspensions were added to HEK-293T cells. At these same time points, hydrogel disks were digested with 10 units/ml alginate lyase (Sigma Aldrich) followed by 50mM EDTA (Sigma Aldrich), the resulting digest was diluted with DMEMc, and the final suspension was then split between HEK-293T cells (final MOI=10). Treated cells were cultured for three days and the transduction efficiency was then measured using flow cytometry (n=3). The data was fit to a one-phase decay fit and the half-life was calculated using Prism 6 software (Graphpad).

Viral vector stability in different pH conditions

AAV and LV suspensions were pre-incubated in media with adjusted pH values of 5, 7.5, and 10 for 1.5 hours. The viral suspensions were then diluted with DMEMc to a neutral pH level and the resulting suspensions were applied to HEK-293T cells (final MOI = 10) and cellular culture was continued for three days. The transduction efficiency of the pH-treated vectors was then measured using flow cytometry (n=3), and values were normalized to neutral pH values for each vector.

Quantification of vector release from alginate hydrogels

Alginate hydrogel disks of both slow and fast degradation formulations were loaded with MOI = 10 of either LV or AAV. Hydrogels were placed in empty 24-well plates, submerged in DMEMc, and incubated at 37˚C and 5% CO_2. Every 24 hours over the course of 5 days, media surrounding each disk was collected was replaced with a fresh

volume. At the end of the 5 days the remaining gels were digested with 10 units/ml alginate lyase followed by 50mM EDTA. The positive control used was DMEMc loaded with MOI=10 of either AAV or LV, and the negative control used was DMEMc alone. Slow and fast hydrogel formulations loaded with LV or AAV were digested with alginate lyase and EDTA immediately after gelation to determine encapsulation efficiency. All samples were stored immediately following collection at -20˚C until analysis by either ELISA (LV) (n=4) or real time PCR (AAV) (n=3 to 4). The LV quantification was performed via ELISA. Specifically, Concentrations of LV within the collected samples were quantified using a HIV p24 ELISA Kit (ZeptoMetrix Co) according to the manufacture's protocol and as previously described (1,16)**.** Following the best practices for AAV quantification, the amount of released AAV was evaluated via real time PCR. Briefly, viral DNA was extracted from AAV capsids using Qiamp Kit (Qiagen) and a quantitative real time PCR assay was performed using Fast SYBR Green Master Mix (Applied Biosystems) in a QuantStudio5 (Applied Biosystems). Preparation of samples was conducted in accordance with manufacturer's protocols. The primers were designed using Primer3 (NCBI Primer-BLAST) and the sequences obtained were eGFP_F: 5'-CACATGAAGCAGCACGACTT-3' and eGFP_R: 5'-GGTCCTGTAGTTGCCGTCGT-3'.

Transduction following release

AAV or LV (MOI=10) were encapsulated in either slow degradation or fast degradation formulation hydrogel disks and placed within 24-well plates seeded with HEK-293T cells. After 24 hours, the disks were recovered and transferred to new wells freshly seeded with HEK-293T cells. In this manner, a series of fresh HEK-293T cells

each endured a 24-hour exposure to the viral-loaded hydrogels over 4 days of viral vector release. Cells from each timepoint were cultured for a full 3 days, and the transduction achieved during the 24-hour hydrogel contact period was measured by flow cytometry (n=4).

Statistical analysis

All statistical analyses were performed using Student's t-tests (two-tail comparisons) or one-way and two-way analysis of variance (ANOVA) with post hoc Tukey's test unless stated otherwise, and analyzed using Prism 6 software (Graphpad). Differences between conditions were considered significant if $P < 0.05$.

RESULTS AND DISCUSSION

In this article, we directly compared two commonly used viral vectors, LV and AAV, in their potential for controlled delivery from alginate hydrogels. Alginate hydrogels have previously been shown capable of delivering a variety of viral vectors with beneficial effects of avoiding vector-specific immune response (1,26), extending the thermal half-life and providing better coverage of targeted tissue coverage while still avoiding off-target expression (1,27). We have previously explored the delivery of LV from alginate hydrogels and alginate hydrogels (1,15). To our knowledge, there have not been any studies that have looked at AAV delivery from degradable alginate hydrogels, however similar strategies have been employed using fibrin (7), PEG (9,28), alginate/poloxamer composite (29), and self-assembling peptide hydrogels (11). Furthermore, a direct side by side comparison of the encapsulation and release of these vectors from alginate hydrogels, or any other hydrogel system, has not been performed. These vectors have key differences in their physical composition, mechanisms of gene delivery, and environmental tolerances that will affect how biomaterial systems should be designed for their controlled release. Here, we demonstrate that the initial strength and degradation rate of alginate hydrogels provides levers of control for tuning LV release but do not provide control in the release of AAV – a schematic of which can be seen in Figure 1A.

Transduction and gene expression profile

We transduced cells with three levels of MOI (20, 10, and 2) for AAV and LV to determine how transduction efficiency varies with vector concentration and to assess the maintenance of gene expression with continuing cell division in culture (Fig. 1B). Near to

100% of cells were transduced using a MOI of 20 for both vectors. However, reducing the vector concentration led to a pronounced drop in transduction efficiency for AAV in comparison to LV. Using a MOI of 2, the transduction efficiency for LV was 56±3% whereas AAV yielded only 20±3%. Continuous culture and cellular expansion for an additional three days also led to a drop in BFP positive cells from AAV transduction. The expansion of cells transduced with a MOI of 20 led to a drop in BFP expression from 92±1% to 46±4%. In comparison, DsRed cells from LV transduction increased in expression for all MOI tested with an increase from 91±2% to 98±0.2% for an MOI of 20.

LV and AAV differ in functional and physical characteristics that will impact their suitability for a given controlled release system. Functionally, these vectors differ in their capacity for gene integration and the duration of gene expression. Transgenes from LV delivery are integrated into the host chromosome, which leads to long-term expression and permanent modification but raises the possibility of insertional mutagenesis (30). The integration of the transgene allows lentivectors to transduce dividing cells without a loss of gene expression as was seen in the continuous culture of HEK-293T after transduction. LV is therefore a useful vector for the transduction of proliferative cells, such as in hematopoietic-stem-cell gene therapy (31). In comparison, AAV remains primarily episomal with low occurrence of integration (5). Accordingly, cellular division is expected to dilute the copies of the delivered gene as was seen for AAV in the dividing HEK-293T cells. In practice, these vectors are commonly used *in vivo* to treat tissue with low cellular turnover where dilution of the episomal gene copies would not be significant (31).

Viral vector response to environmental conditions

We incubated viral vector suspensions and viral-loaded hydrogels in DMEMc at 37˚C and analyzed transduction efficiency with increasing incubation time and altered media pH (Fig. 2A). LV displayed the quickest reduction in transduction efficiency at a neutral pH with a half-life of 25 hours in suspension and 14 hours for encapsulation and digestion. In comparison, AAV displayed a minimal loss in transduction efficiency over 2 days in both suspension and encapsulation and did not fit to a one-phase decay model. The two vectors displayed markedly different tolerance to environmental pH adjustments (Fig. 2B). AAV remained stable at all pH levels tested and displayed a 1.4±0.2 fold increase over the neutral pH control after incubation in acidified media. Conversely, LV was susceptible to both acidic and basic conditions with respective reductions to 0.56±0.05 and 0.78±0.07 of the neutral pH control.

The loss of activity for LV over time at 37˚C is consistent with loss of infectivity due to thermal degradation of virus particles (32,33). Furthermore, encapsulation and release via digestion exacerbated the decay of transduction efficiency for LV. However, this may in part be due to the gelation route chosen as the pH of $CaCO_3$-GDL hydrogels is expected to be slightly acidic (15). This drop in pH is minimal due to the buffering capacity of the carbonate, but the vectors were held in these encapsulation conditions for prolonged periods of time which may worsen any detrimental effect. In practice, many encapsulation strategies rely on adjustments of pH. Exposure to weak acids can be used in alginate hydrogels to release calcium on-demand from pH-sensitive sequestered forms such as calcium carbonate (34,35) or chelated complexes (36,37). These sequestered cation sources can provide control over gelation kinetics and shape manipulation of

alginate hydrogels (34). However, these gelation strategies may be more suitable for AAV than for LV based on the results seen here and in previous work (38,39).

Hydrogel strength and degradation

The two alginate formulations used, slow and fast degradation formulations, yielded hydrogel disks with drastically different initial strengths and degradation rates. Initially, both hydrogels formed into disks of similar mass (Fig. 3A), however the slow degradation formulation hydrogels possessed a 5.8-fold higher storage modulus compared to fast degradation formulation hydrogels (Fig. 3C). Average initial mesh sizes were 123nm and 273nm were calculated for the slow and fast degradation formulations, respectively (Fig. 3E). The profiles of mass loss, storage modulus loss, and mesh size change over time in incubation were drastically different between the two formulations (Fig. 3B, 3D, and 3F respectively). Fast degradation formulation hydrogels lost 98% of the initial storage modulus and showed increased mesh sizes within the first 12 hours and completely degraded within 24 hours where there was no recoverable dry mass. Contrasting this rapid structural change, slow degradation formulation hydrogels maintained 50% of the initial storage modulus after 1 day in incubation, and then gradually lost mechanical strength over 60 days while generally maintaining mesh size.

This difference in strength and degradation rates is in agreement with previous findings, as it has been shown that a high level of oxidation, as used in the fast degradation alginate formulation, leads to a dramatic drop in hydrogel strength, and produces a hydrogel with larger initial mesh size and faster degradation over time (24). In comparison, lower levels of oxidation, as used here in the slow degradation formulation,

do not decrease hydrogel strength to the same extent and promotes gradual degradation over the course of weeks (40).

Vector release from hydrogel disks

The release profile of LV and AAV from slow and fast degradation hydrogel formulations was assessed by using ELISA and real time PCR respectively. On average for both vectors, the slow degradation formulation hydrogels had an encapsulation efficiency of 40%, and the fast degradation formulation hydrogels had encapsulation efficiency of 65%. The slow hydrogel formulation released a total of 20% of the loaded LV within 5 days, which is a significant difference when compared to the fast degradation formulation hydrogel formulation, that released 44% of the loaded LV payload within the same period of time (Fig. 4B). In contrast, both slow and fast degradation formulation alginate hydrogels released AAV particles at a consistent rate over 5 days, releasing 80% and 84% of their loaded AAV particles, respectively (Fig. 4A). This illustrates that LV release was dependent on the hydrogel formulations used in this study, while AAV release was independent. Furthermore, this suggests the larger LV particle requires hydrogel degradation to release vectors into solution, while the smaller AAV particle's release is mainly dependent on a diffusive mechanism. Noteworthy, fast degradation formulation hydrogels in this release study did not experience complete degradation within 24 hours like other fast degradation formulation hydrogels - possibly due to differences in the long-term storage of the alginates used. Significantly, however, trends of release and release rate were consistent with prior figures of this work.

Homogenous dispersion of viral particles within the alginate hydrogel disks of both slow and fast degradation formulations were obtained by thoroughly mixing viral particles into alginate polymer solutions prior to the addition of crosslinking agents. Importantly, the physical nature of both the vectors used and of the hydrogel employed are key in obtaining a given profile of release. Broadly speaking, the release of encapsulated cargo from hydrogels is highly dependent on the relative size of the encapsulated therapeutic and the mesh size of the hydrogel (23). The differences in release are explainable by the relative hydrodynamic radii and surface features of these vectors, and are in agreement with previous reports of particle encapsulation and controlled release from hydrogels (22,23). Cargo that is smaller than the mesh size of the hydrogel can rely on diffusive release, whereas larger cargo is sufficiently immobilized to necessitate either deformation, swelling, or degradation of the hydrogel to facilitate release (22,23). LV vectors are particles with a reported hydrodynamic radius of 166 nm and possess an enveloped capsid (41). AAV particles in comparison are substantially smaller, with a non-enveloped capsid hydrodynamic radius of 29 nm (31). Accordingly, the release of the larger LV particles, but not the small AAV particles, from hydrogels was shown to be highly dependent on the formulation of alginate in which the vector was encapsulated, while AAV release is mainly reliant on a diffusive mechanism.

Transduction following release from alginate hydrogel disks

While it has been shown that viral vectors were released from both slow and fast degradation hydrogel formulations (Fig. 4), to ensure the activity of the vectors being released, transduction studies using the same disk dimensions and viral MOI were

performed. Hydrogels were loaded with a MOI = 10 of either LV or AAV and placed in contact with a series of HEK-293T cells over four days. Hydrogel disks were moved to new HEK-293T cells every 24 hours to capture the profile of release of functional vectors. Fluorescent microscopy documents that functional viral vectors successfully escaped encapsulation and transduced cells in the first 24 hours, however this release was vector and formulation specific (Fig. 5A). Fast degradation formulation hydrogels were required to observe substantial fluorescence for LV, whereas BFP fluorescence from AAV was visible from both the slow degradation and fast degradation formulation hydrogel systems. These early time point trends were confirmed with flow cytometry analysis (Fig. 5B). Low levels of transduction, 2.1%±0.7% DsRed+ cells, were achieved for cells exposed to LV loaded within slow degradation formulation hydrogels. This same alginate formulation yielded significantly higher transduction, 28±5% BFP+ cells, when loaded with AAV. In contrast, both the LV loaded and AAV loaded fast degradation formulation alginate hydrogels promoted significant transduction with 40%±4% DsRed+ cells and 37%±5%BFP+ cells respectively. In time points following this initial 24 hours there was little transduction from both alginate formulations and vector type.

LV showed little transduction from the slow degradation formulation, but was capable of promoting transduction from the fast degradation formulation hydrogel. The rapid degradation of this hydrogel formulation increases the mesh size to an extent that the vector is free to release and transduce cells. Therefore, hydrogel delivery systems should be designed for LV that promote release from their steric entrapment. In comparison, AAV was successfully released from both formulations and delivered the transgene of interest. This result suggests that the AAV vector is capable of diffusive

transport from the alginate mesh, and implies that the mesh size may be on the same order of magnitude as the AAV vector. To gain sufficient control in AAV delivery it will be necessary to design hydrogels that limit the initial burst release observed. Burst release from alginate hydrogels can be modulated in several ways. For example, increasing alginate hydrogel strength decreases the release rate of payloads and can be achieved by increasing the molecular weight of alginate used, increasing the alginate content of the gels, and decreasing or eliminating oxidation (22,24,25,40). In alternative, increasing hydrogel strength decreases mesh and pore sizes of the gels, and thus decreases the rate of payload release (22,24,25,40). However such modifications, collectively, are likely to jeopardize the ability to use these alginate hydrogels as injectable vehicles. In addition, alginate hydrogels could also be modified with specific cell anchoring peptides that further enhance alginate ability to interact with small molecules and cells (10,17,18). Since AAV has shown preferential affinity for select cell surface receptors depending on the serotype (42), it may be possible to harness these interactions through peptide modification of alginate hydrogels.

CONCLUSIONS

In this study, we validated the potential of two viral vectors, LV and AAV, to promote transgene expression following release from alginate hydrogels. In doing so, we have identified key differences between the vectors that govern how release systems would need to be designed to optimize gene delivery. To our knowledge this is the first demonstration of AAV delivery from a degradable alginate-based system. With the growing interest in LV and AAV therapies, alginate hydrogel delivery may be valuable in

the development of spatiotemporal controls to increase the localization and efficiency of gene therapies.

ACKNOWLEDGEMENTS

We would like to thank Prof. Jamal Lewis' (UC Davis) group for their support with flow cytometry experiments. We kindly express our gratitude to Prof. Julie Bossuyt's group (UC Davis) for their outstanding support in producing the lentivectors. We thank the UC Davis College of Engineering and the National Science Foundation (NSF) Scholarship in Science Technology Engineering and Mathematics Program for their funding support (SS). Finally, we thank the American Heart Association (17IRG33420114) for the funding support for this work.

DISCLOSURES

None.

Vector	Hydrodynamic Radius (nm)	Zeta Potential (mV)	Envelope	Viral Gene Presence in Cell
Adeno-associated Vector	**29** (43)	**-9** (30)	**-** (43)	**Episomal** (5)
Lentivector	**166** (41)	**-18**(30)	**+** (41)	**Integrative** (1)

Table 1: Key characteristics of lentivectors and adeno-associated vectors.

FIGURE LEGENDS

Figure 1: Experimental scheme and transduction of HEK-293T at different MOI. An illustration depicting the putative mechanism of release for the two viral vectors from degradable alginate hydrogels (A). LV and AAV achieve high transduction efficiency at MOI of 20 as measured using flow cytometry (n=3) (B). However, the AAV used exhibits a drop in efficiency when the transducing concentration is lowered. Furthermore, the cellular division occurring in culture over 6 days is sufficient to dilute the expression of AAV for all MOI used. Bars represent mean with individual measurements denoted by scatter points and the error bars indicates standard deviation.

Figure 2: Viral vector stability. The stability of the two vectors in cell-culture conditions varies dramatically in both free suspension (solid lines, close symbols) and encapsulation (dashed lines, open symbols) as measured by flow cytometry as shown in one-phase decay models (n = 3) (A). LV in suspension and encapsulation has R^2 values of 0.89 and 0.98, respectively, and displays a marked drop in transduction efficiency over two days which is exacerbated by encapsulation and digestion. AAV, in contrast, has R^2 values of 0.17 and 0.23 in suspension and encapsulation, respectively, and remains relatively stable in these conditions with minimal loss in transduction efficiency after 2 days. The two vectors were exposed to both acidic and basic environments prior to cellular exposure and the transduction efficiency was quantified by flow cytometry (n=3). Data was normalized to neutral pH values for each vector (B). LV transduction efficiency was decreased at both pH 5 and pH 10 in comparison to neutral pH. In contrast, AAV maintained transduction potential throughout the pH ranges tested and promoted the

highest protein expression following exposure to an acidic environment. Bars represent mean with individual measurements denoted by scatter points and the error bars indicates standard deviation. Asterisk (*) specify statistically significant differences ($P < 0.05$) between conditions.

Figure 3: Mechanical characterization of alginate hydrogels. Hydrogels formulated using both slow and fast degradation compositions yielded disks of similar mass (n=8 for both slow and fast degradation formulations) (A), however, dry mass loss over time illustrates the degradation differences of the two gel formulations (n=6 to 8 for both slow and fast degradation formulations) (B). Slow and fast gel formulations differed in their initial strength, as shown by their storage moduli both initially (n=6, n=8; slow and fast degradation formulations, respectively) (C), and over time (n=6 to 8, n=8; slow and fast degradation formulations, respectively) (D) and their mesh sizes both initially (n=8 for both slow and fast degradation formulations) (E) and over time (n=6 to 8, n=4 to 8 for slow and fast degradation formulations, respectively) (F). Fast degradation formulation hydrogels completely fell apart within 24 hours whereas the slow degradation formulation hydrogels lost strength over the course of 60 days. Bars represent mean with individual measurements denoted by scatter points and the error bars indicates either standard deviation for graphs A through D and propagation of error of swelling ratio of wet mass over dry mass (Q_m) and storage modulus (G') in graphs E and F. Shaded areas denote the error envelope and represents standard deviation (A – D) or propagation of error (E – F). Asterisk (*) indicates statistically significant differences ($P < 0.05$) between conditions.

Figure 4: Release profiles of viral vectors from degradable hydrogel disks. AAV release profiles of both slow and fast degradation formulations as determined by qPCR of viral DNA (n=3 to 4) are similar in both magnitude and trend (A). In contrast, the LV release kinetics as determined by ELISA (n=4) showed that slow and fast degradation formulations presented two different profiles of release over the time (B). Fast degradation formulation hydrogels delivered more than twice the amount of LV in comparison to slow degradation formulation hydrogels in the same time. The mean is represented by the central line, and the shaded areas denote the error envelope and represents the standard deviation.

Figure 5: Transduction following release from degradable hydrogel disks. Composite phase-contrast and fluorescent images are shown for expression achieved after the first day of contact with the viral-loaded disks. AAV (expressing BFP – blue) was capable of escape from both hydrogel systems, whereas the fast degradation formulation hydrogel was required for significant fluorescence to be observed for LV (expressing DsRed – red) (A). Viral-loaded hydrogels were exposed to new sets of cells every 24 hours. The transduction efficiency at each time point was assessed after 3 days of culture by flow cytometry (B). Scale bars represent 100μm. Bars represent mean with individual measurements denoted by scatter points and the error bars indicates standard deviation.

REFERENCES

1. Stilhano RS, Madrigal JL, Wong K, Williams PA, Martin PKM, Yamaguchi FSM, et al. Injectable alginate hydrogel for enhanced spatiotemporal control of lentivector delivery in murine skeletal muscle. J Control Release Off J Control Release Soc. 2016 10;237:42–9.

2. Naldini L, Blömer U, Gallay P, Ory D, Mulligan R, Gage FH, et al. In vivo gene delivery and stable transduction of nondividing cells by a lentiviral vector. Science. 1996 Apr 12;272(5259):263–7.

3. Christodoulou I, Patsali P, Stephanou C, Antoniou M, Kleanthous M, Lederer CW. Measurement of lentiviral vector titre and copy number by cross-species duplex quantitative PCR. Gene Ther. 2016 Jan;23(1):113–8.

4. Pluta K, Kacprzak MM. Use of HIV as a gene transfer vector. Acta Biochim Pol. 2009;56(4):531–95.

5. Lai CM, Lai YKY, Rakoczy PE. Adenovirus and Adeno-Associated Virus Vectors. DNA Cell Biol. 2002 Dec 1;21(12):895–913.

6. Boutin S, Monteilhet V, Veron P, Leborgne C, Benveniste O, Montus MF, et al. Prevalence of serum IgG and neutralizing factors against adeno-associated virus (AAV) types 1, 2, 5, 6, 8, and 9 in the healthy population: implications for gene therapy using AAV vectors. Hum Gene Ther. 2010 Jun;21(6):704–12.

7. Lee HH, Haleem AM, Yao V, Li J, Xiao X, Chu CR. Release of Bioactive Adeno-Associated Virus from Fibrin Scaffolds: Effects of Fibrin Glue Concentrations. Tissue Eng Part A. 2011 Aug;17(15–16):1969–78.

8. Raut SD, Lei P, Padmashali RM, Andreadis ST. Fibrin-mediated lentivirus gene transfer: Implications for lentivirus microarrays. J Controlled Release. 2010 Jun;144(2):213–20.

9. Zeng Y-F, Tseng S-J, Kempson IM, Peng S-F, Wu W-T, Liu J-R. Controlled delivery of recombinant adeno-associated virus serotype 2 using pH-sensitive poly(ethylene glycol)-poly-L-histidine hydrogels. Biomaterials. 2012 Dec;33(36):9239–45.

10. Seidlits SK, Gower RM, Shepard JA, Shea LD. Hydrogels for lentiviral gene delivery. Expert Opin Drug Deliv. 2013 Apr;10(4):499–509.

11. Rey-Rico A, Venkatesan JK, Frisch J, Schmitt G, Monge-Marcet A, Lopez-Chicon P, et al. Effective and durable genetic modification of human mesenchymal stem cells via controlled release of rAAV vectors from self-assembling peptide hydrogels with a maintained differentiation potency. Acta Biomater. 2015 May;18:118–27.

12. Rodriguez AL, Wang T-Y, Bruggeman KF, Li R, Williams RJ, Parish CL, et al. Tailoring minimalist self-assembling peptides for localized viral vector gene delivery. Nano Res. 2016 Mar;9(3):674–84.

13. Aikawa T, Ito S, Shinohara M, Kaneko M, Kondo T, Yuasa M. A drug formulation using an alginate hydrogel matrix for efficient oral delivery of the manganese porphyrin-based superoxide dismutase mimic. Biomater Sci. 2015 May 19;3(6):861–9.

14. Gentile P, Ghione C, Ferreira AM, Crawford A, Hatton PV. Alginate-based hydrogels functionalised at the nanoscale using layer-by-layer assembly for potential cartilage repair. Biomater Sci. 2017 Aug 22;5(9):1922–31.

15. Madrigal JL, Stilhano RS, Siltanen C, Tanaka K, Rezvani SN, Morgan RP, et al. Microfluidic generation of alginate microgels for the controlled delivery of lentivectors. J Mater Chem B. 2016;4(43):6989–99.

16. Madrigal JL, Sharma SN, Campbell KT, Stilhano RS, Gijsbers R, Silva EA. Microgels produced using microfluidic on-chip polymer blending for controlled released of VEGF encoding lentivectors. Acta Biomater. 2018 Mar 15;69:265–76.

17. Silva EA, Kim E-S, Kong HJ, Mooney DJ. Material-based deployment enhances efficacy of endothelial progenitor cells. Proc Natl Acad Sci U S A. 2008 Sep 23;105(38):14347–52.

18. Rowley JA, Mooney DJ. Alginate type and RGD density control myoblast phenotype. J Biomed Mater Res. 2002 May;60(2):217–23.

19. Coviello T, Matricardi P, Alhaique F. Drug delivery strategies using polysaccharidic gels. Expert Opin Drug Deliv. 2006 May;3(3):395–404.

20. Kong HJ, Kim ES, Huang Y-C, Mooney DJ. Design of Biodegradable Hydrogel for the Local and Sustained Delivery of Angiogenic Plasmid DNA. Pharm Res. 2008 May;25(5):1230–8.

21. Grassi M, Sandolo C, Perin D, Coviello T, Lapasin R, Grassi G. Structural Characterization of Calcium Alginate Matrices by Means of Mechanical and Release Tests. Molecules. 2009 Aug 12;14(8):3003–17.

22. Li J, Mooney DJ. Designing hydrogels for controlled drug delivery. Nat Rev Mater. 2016 Dec;1(12).

23. De Laporte L, Shea LD. Matrices and scaffolds for DNA delivery in tissue engineering. Adv Drug Deliv Rev. 2007 May 30;59(4):292–307.

24. Bouhadir KH, Lee KY, Alsberg E, Damm KL, Anderson KW, Mooney DJ. Degradation of partially oxidized alginate and its potential application for tissue engineering. Biotechnol Prog. 2001 Oct;17(5):945–50.

25. Kong HJ, Kaigler D, Kim K, Mooney DJ. Controlling rigidity and degradation of alginate hydrogels via molecular weight distribution. Biomacromolecules. 2004 Oct;5(5):1720–7.

26. Sailaja G, HogenEsch H, North A, Hays J, Mittal SK. Encapsulation of Recombinant Adenovirus into Alginate Microspheres Circumvents Vector Specific Immune Response. Gene Ther. 2002 Dec;9(24):1722–9.

27. Choi J-W, Kang E, Kwon O-J, Yun TJ, Park H-K, Kim P-H, et al. Local sustained delivery of oncolytic adenovirus with injectable alginate gel for cancer virotherapy. Gene Ther. 2013 Sep;20(9):880–92.

28. Tseng S-J, Kempson IM, Peng S-F, Ke B-H, Chen H-H, Chen P-F, et al. Environment acidity triggers release of recombinant adeno-associated virus serotype 2 from a tunable matrix. J Control Release Off J Control Release Soc. 2013 Sep 10;170(2):252–8.

29. Díaz-Rodríguez P, Rey-Rico A, Madry H, Landin M, Cucchiarini M. Effective genetic modification and differentiation of hMSCs upon controlled release of rAAV vectors using alginate/poloxamer composite systems. Int J Pharm. 2015 Dec;496(2):614–26.

30. Madrigal JL, Stilhano R, Silva EA. Biomaterial-Guided Gene Delivery for Musculoskeletal Tissue Repair. Tissue Eng Part B Rev. 2017 Feb 6;23(4):347–61.

31. Naldini L. Gene therapy returns to centre stage. Nature. 2015 Oct 15;526(7573):351–60.

32. Higashikawa F, Chang L-J. Kinetic Analyses of Stability of Simple and Complex Retroviral Vectors. Virology. 2001 Feb 1;280(1):124–31.

33. Pelliccia M, Andreozzi P, Paulose J, D'Alicarnasso M, Cagno V, Donalisio M, et al. Additives for vaccine storage to improve thermal stability of adenoviruses from hours to months. Nat Commun. 2016 Nov 30;7:13520.

34. Kuo CK, Ma PX. Ionically crosslinked alginate hydrogels as scaffolds for tissue engineering: part 1. Structure, gelation rate and mechanical properties. Biomaterials. 2001 Mar;22(6):511–21.

35. Kuo CK, Ma PX. Maintaining dimensions and mechanical properties of ionically crosslinked alginate hydrogel scaffolds in vitro. J Biomed Mater Res A. 2008 Mar 15;84(4):899–907.

36. G. Håti A, C. Bassett D, M. Ribe J, Sikorski P, A. Weitz D, T. Stokke B. Versatile, cell and chip friendly method to gel alginate in microfluidic devices. Lab Chip. 2016;16(19):3718–27.

37. Utech S, Prodanovic R, Mao AS, Ostafe R, Mooney DJ, Weitz DA. Microfluidic Generation of Monodisperse, Structurally Homogeneous Alginate Microgels for Cell Encapsulation and 3D Cell Culture. Adv Healthc Mater. 2015 Aug 5;4(11):1628–33.

38. Gruntman AM, Su L, Su Q, Gao G, Mueller C, Flotte TR. Stability and Compatibility of Recombinant Adeno-Associated Virus Under Conditions Commonly Encountered in Human Gene Therapy Trials. Hum Gene Ther Methods. 2015 Mar 27;26(2):71–6.

39. Hoggan MD, Blacklow NR, Rowe WP. Studies of small DNA viruses found in various adenovirus preparations: physical, biological, and immunological characteristics. Proc Natl Acad Sci U S A. 1966 Jun;55(6):1467–74.

40. Boontheekul T, Kong H-J, Mooney DJ. Controlling alginate gel degradation utilizing partial oxidation and bimodal molecular weight distribution. Biomaterials. 2005 May;26(15):2455–65.

41. Croyle MA, Callahan SM, Auricchio A, Schumer G, Linse KD, Wilson JM, et al. PEGylation of a vesicular stomatitis virus G pseudotyped lentivirus vector prevents inactivation in serum. J Virol. 2004 Jan;78(2):912–21.

42. Nonnenmacher M, Weber T. Intracellular transport of recombinant adeno-associated virus vectors. Gene Ther. 2012 Jun;19(6):649–58.

43. Wright JF, Le T, Prado J, Bahr-Davidson J, Smith PH, Zhen Z, et al. Identification of factors that contribute to recombinant AAV2 particle aggregation and methods to prevent its occurrence during vector purification and formulation. Mol Ther. 2005 Jul 1;12(1):171–8.

Figure 1

A)

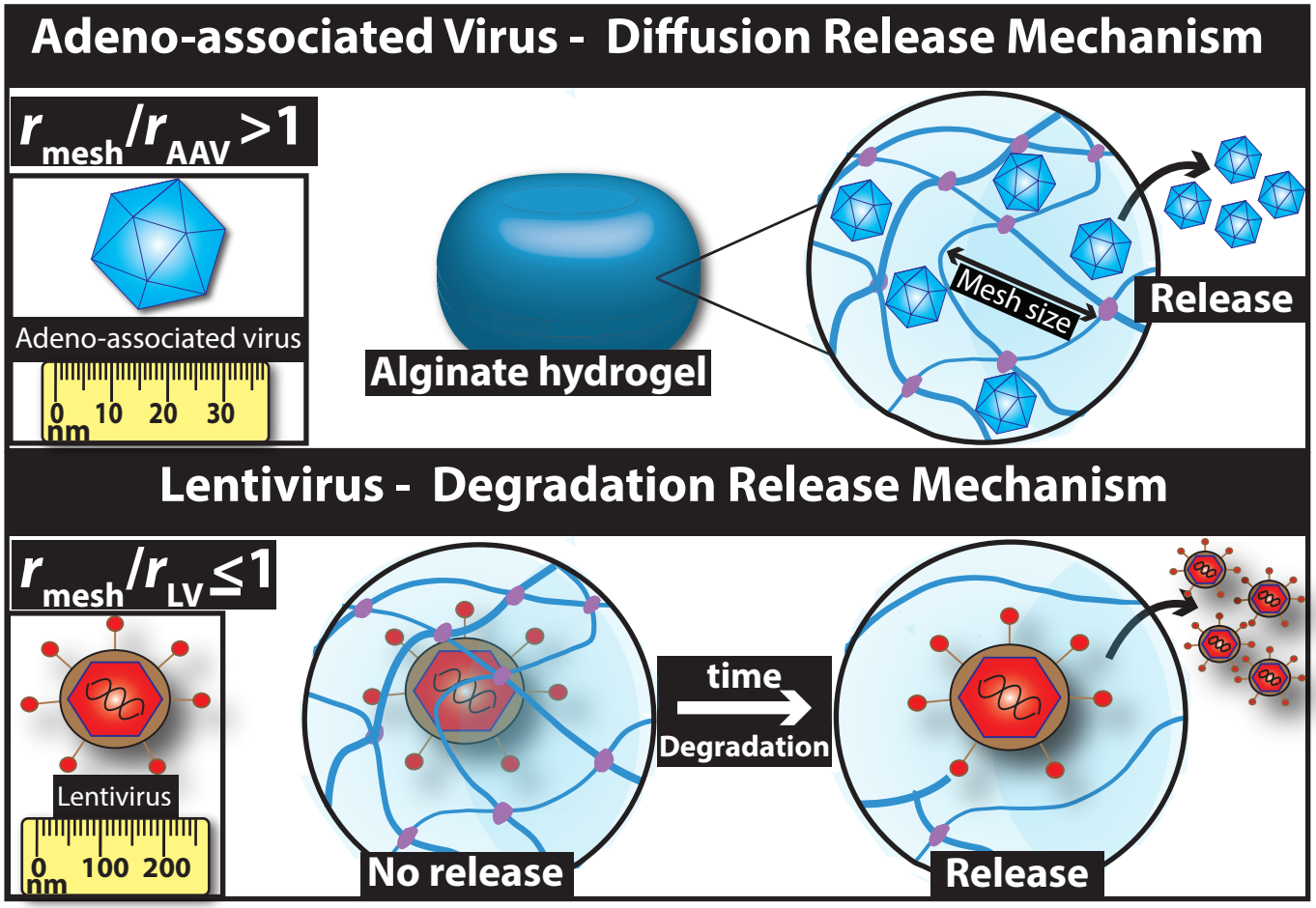
Adeno-associated Virus - Diffusion Release Mechanism
$r_{mesh}/r_{AAV} > 1$
Adeno-associated virus
0 10 20 30 nm
Alginate hydrogel
Mesh size
Release
Lentivirus - Degradation Release Mechanism
$r_{mesh}/r_{LV} \leq 1$
Lentivirus
0 100 200 nm
No release
time
Degradation
Release

B)

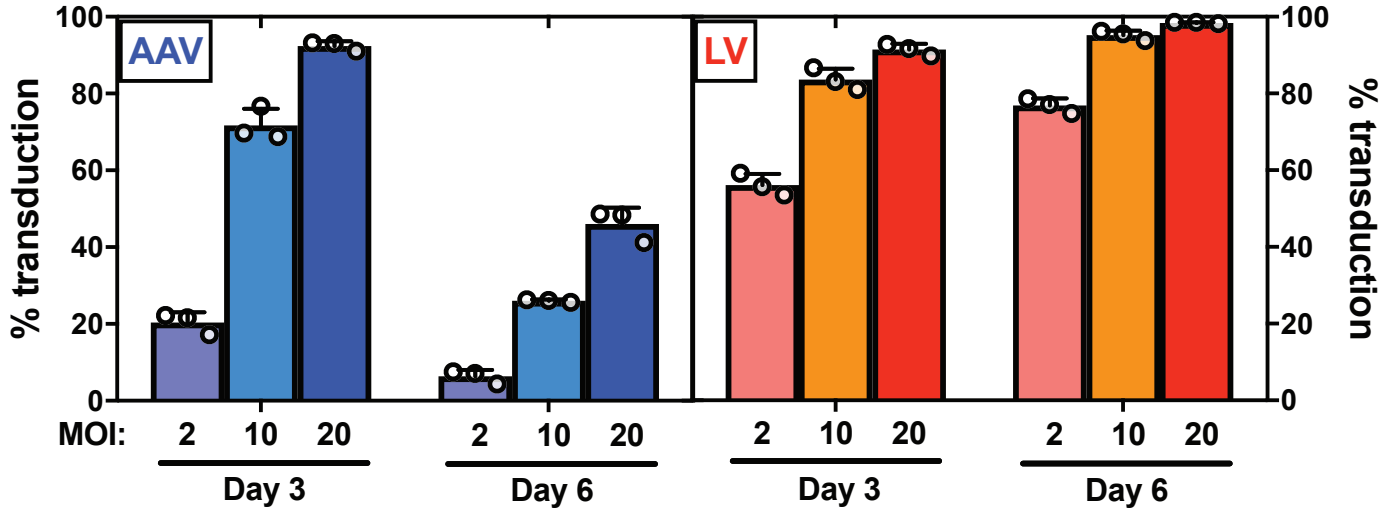
AAV
LV
% transduction
100
80
60
40
20
0
MOI: 2 10 20
Day 3
Day 6

Figure 2

A)

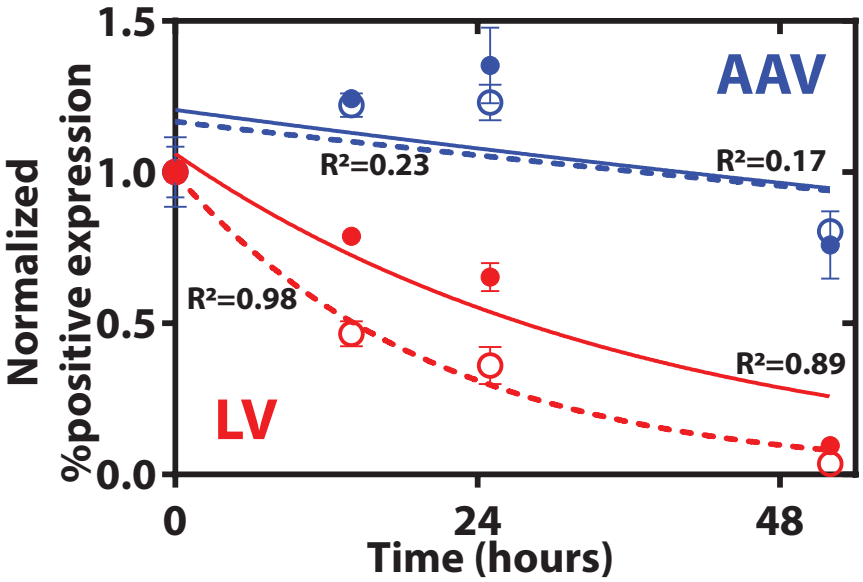
1.5
1.0
0.5
0.0
Normalized
%positive expression
AAV
R²=0.23
R²=0.17
R²=0.98
R²=0.89
LV
0
24
48
Time (hours)

B)

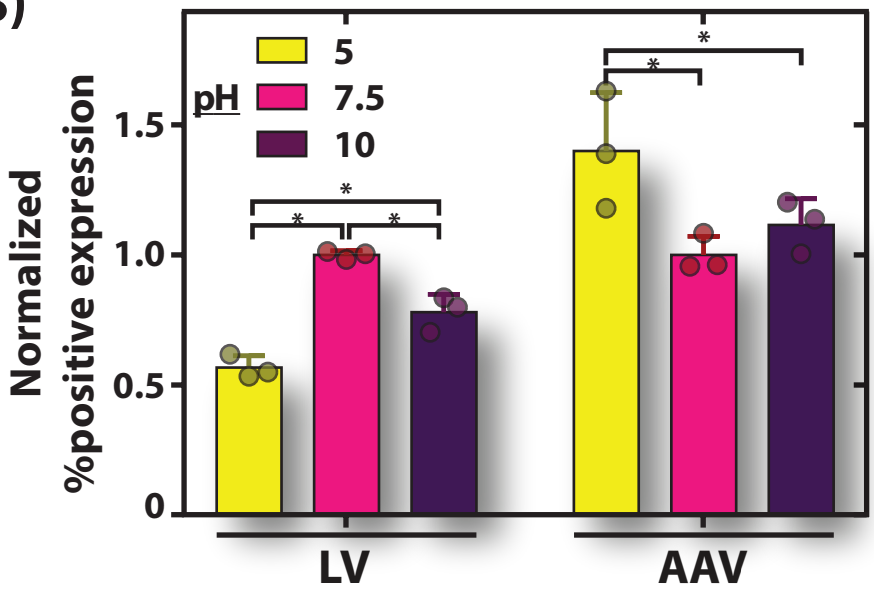
pH
5
7.5
10
*
*
*
*
1.5
1.0
0.5
0
Normalized
%positive expression
LV
AAV

Figure 3

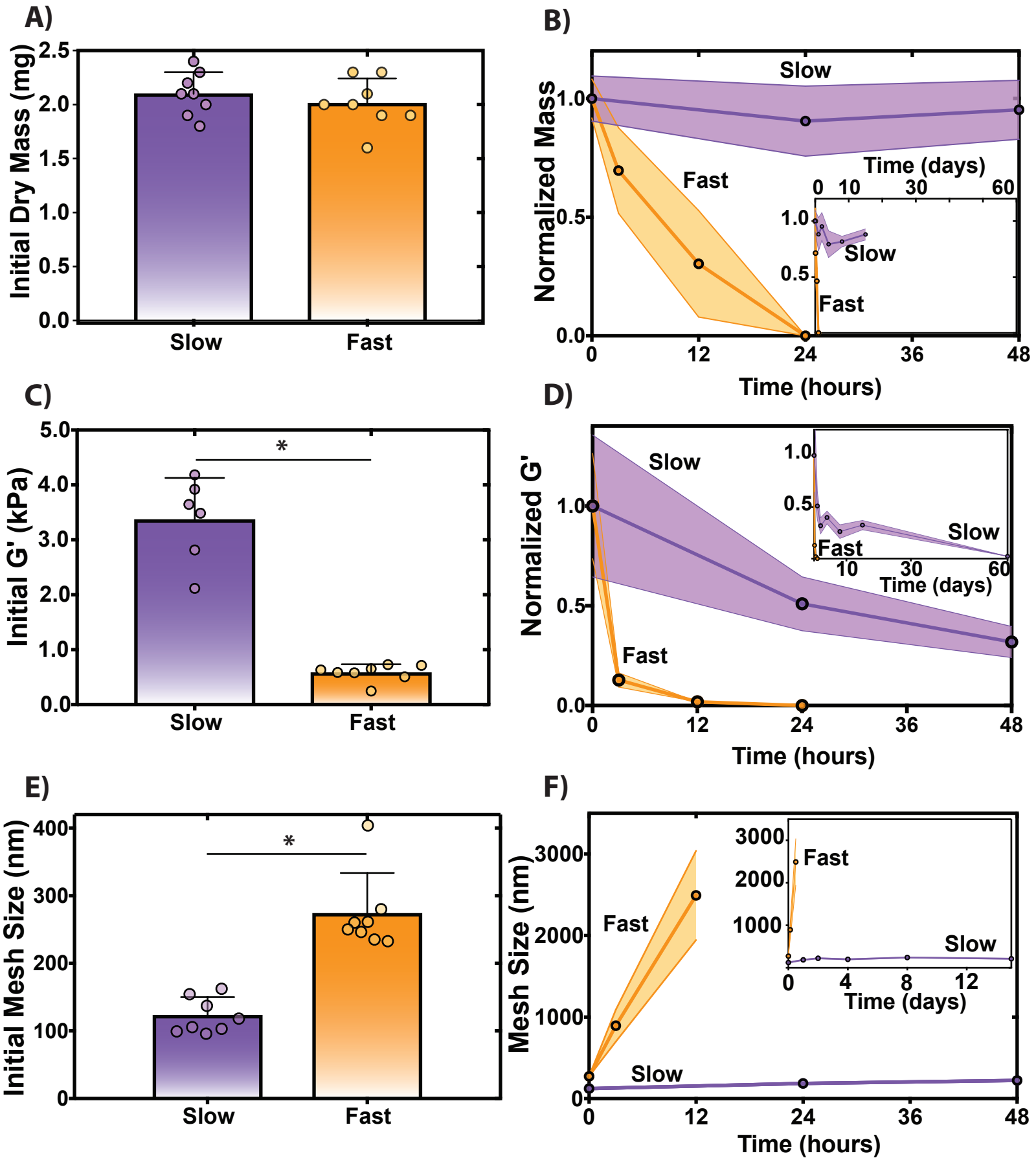
A)
Initial Dry Mass (mg)
2.5
2.0
1.5
1.0
0.5
0.0
Slow
Fast
B)
Normalized Mass
1.0
0.5
0.0
Slow
Fast
Time (days)
0
10
30
60
1.0
0.5
Slow
Fast
0
12
24
36
48
Time (hours)
C)
Initial G' (kPa)
5.0
4.0
3.0
2.0
1.0
0.0
*
Slow
Fast
D)
Normalized G'
1.0
0.5
0.0
Slow
1.0
0.5
Fast
10
30
60
Time (days)
Slow
Fast
0
12
24
36
48
Time (hours)
E)
Initial Mesh Size (nm)
400
300
200
100
0
*
Slow
Fast
F)
Mesh Size (nm)
3000
2000
1000
0
Fast
3000
2000
1000
Fast
Slow
0
4
8
12
Time (days)
Slow
0
12
24
36
48
Time (hours)

Figure 4

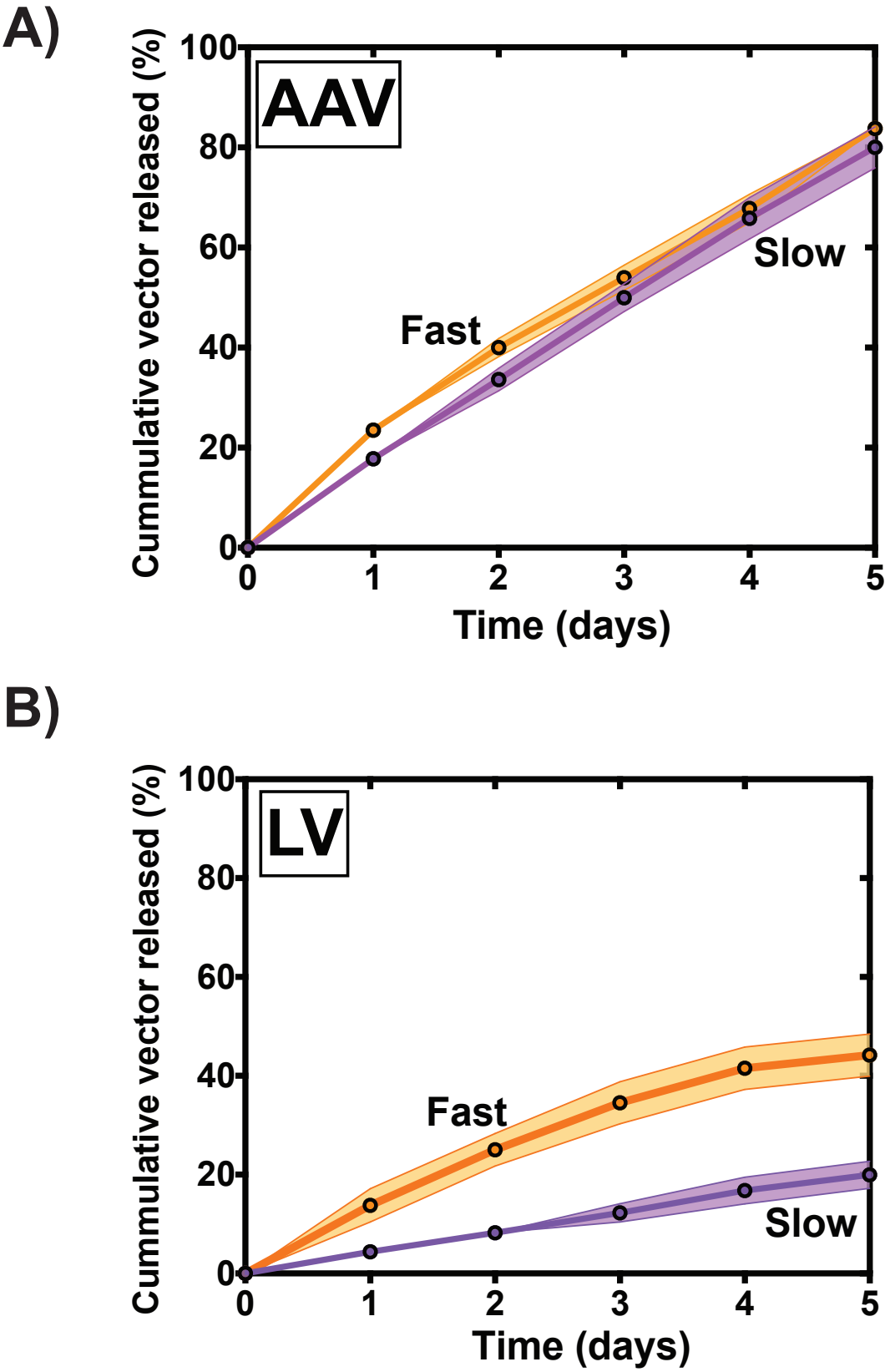
A)
AAV
Cummulative vector released (%)
100
80
60
40
20
0
Fast
Slow
0
1
2
3
4
5
Time (days)
B)
LV
Cummulative vector released (%)
100
80
60
40
20
0
Fast
Slow
0
1
2
3
4
5
Time (days)

Figure 5

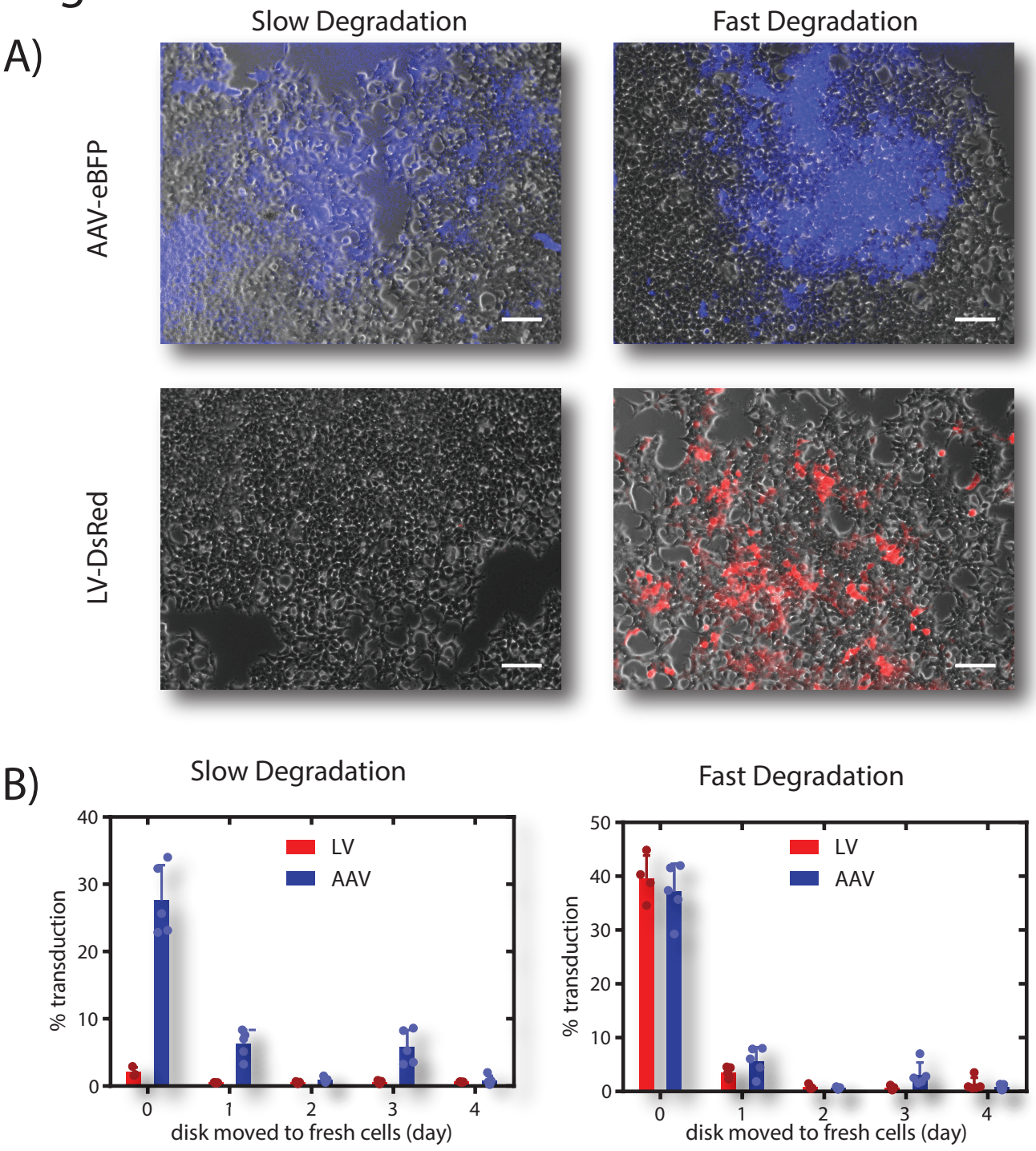
A)
Slow Degradation
Fast Degradation
AAV-eBFP
LV-DsRed
B)
Slow Degradation
Fast Degradation
% transduction
LV
AAV
disk moved to fresh cells (day)
0
10
20
30
40
50
1
2
3
4